Atmospheric
Chemistry
and Physics
Discussions

1   Surface ozone over High-Mountain Asia controlled by stratospheric intrusion

2   Xiufeng Yin [1,2], Dipesh Rupakheti [3], Guoshuai Zhang [4], Jiali Luo [5], Shichang Kang [1,6], Benjamin de Foy [7],

3   Junhua Yang [1], Zhenming Ji [8], Zhiyuan Cong [2,9], Maheswar Rupakheti [10], Ping Li [11], Qianggong Zhang [2,9,*]

4   [1] State Key Laboratory of Cryospheric Science, Northwest Institute of Eco-Environment and Resources, Chinese Academy of
5   Science, Lanzhou 730000, China

6   [2] Key Laboratory of Tibetan Environment Changes and Land Surface Processes, Institute of Tibetan Plateau Research, Chinese
7   Academy of Sciences, Beijing 100101, China

8   [3] Jiangsu Key Laboratory of Atmospheric Environment Monitoring and Pollution Control, Collaborative Innovation Center of
9   Atmospheric Environment and Equipment Technology, School of Environmental Science and Engineering, Nanjing University
10   of Information Science and Technology, Nanjing 210044, China

11   [4] Chinese Academy of Environmental Planning, Beijing 100012, China

12   [5] Key Laboratory for Semi-Arid Climate Change of the Ministry of Education, College of Atmospheric Sciences, Lanzhou
13   University, Lanzhou 730000, China

14   [6] University of Chinese Academy of Sciences, Beijing 100049, China

15   [7] Department of Earth and Atmospheric Sciences, Saint Louis University, St. Louis, MO, 63108, USA

16   [8] School of Atmospheric Sciences, Key Laboratory for Climate Change and Natural Disaster Studies of and Guangdong
17   Province, Sun Yat-sen University, Guangzhou 510275, China

18   [9] State Key Laboratory of Tibetan Plateau Earth System Science, Institute of Tibet Plateau Research, Chinese Academy of
19   Sciences, Beijing 100101, China;

20   [10] Institute for Advanced Sustainability Studies, Potsdam, Germany

21   [11] Key Laboratory of Land Surface Process and Climate Change in Cold and Arid Regions, Northwest Institute of Eco-
22   Environment and Resources, Chinese Academy of Science, Lanzhou 730000, China

23

24

25   *Correspondence to: Qianggong Zhang (qianggong.zhang@itpcas.ac.cn)

26

27

28

29

30

31   **Abstract:**

32   High-Mountain Asia (HMA) is a global hotspot of stratospheric intrusion, and elevated surface ozone were observed at

33   ground monitoring sites. Still, links between the variability of surface ozone and stratospheric intrusion at regional scale remain

34   unclear. This study synthesized ground measurements of surface ozone over the HMA and analyzed their seasonal variations.

35   The monthly mean surface ozone concentrations peaked earlier in the south in April and later in the north in July over the

36   HMA. The migration of monthly surface ozone peaks was coupled with the synchronous movement of tropopause folding and

37   westerly jet that created a conducive conditions for stratospheric ozone intrusion. Such intrusion contributed ~65% of surface

38   ozone at three typical sites across the HMA. We demonstrated that surface ozone over the HMA is mainly controlled by

39   stratospheric intrusion, which warrants a proper consideration in understanding atmospheric chemistry and impacts of ozone

40   over this highland region and beyond.

41

1. Introduction

43   Tropospheric surface ozone (O_3) has attracted great attention during the last decades due to its impact on the oxidative

44   capacity of the troposphere, the radiative forcing of the atmosphere, the detrimental effects on the vegetation and ecosystem,

45   and human health (Crutzen, 1988). The tropospheric (surface) ozone is controlled by in situ photochemical production in the

46   troposphere and by the intrusion of ozone-laden stratospheric air (Crutzen, 1988; Bracci et al., 2012). In contrast with other

47   air pollutants, tropospheric ozone is significantly influenced by stratospheric intrusion, especially at high elevation (Bracci et

48   al., 2012; Cristofanelli et al., 2010; Yin et al., 2017).

49   High-Mountain Asia (HMA) is a geographic region centered at Tibetan Plateau, and includes surrounding cordillera and

50   highland. The Tibetan Plateau (main body of HMA) is a vast plateau with an average elevation of ca. 4,500 m above sea level,

51   making it the highest plateau in the world. It is thus often referred to as "the roof of the world" or "the third pole" (Yao et al.,

52   2012). With limited human accessibility and low levels of industrialization, HMA is one of the most pristine regions in the

53   world in terms of most of the air pollutants (Yin et al., 2017) and is regarded as an ideal area for studying the atmospheric

54   environment in the free troposphere. It can provide deeper insights into changing background concentrations of atmospheric

55   pollutants (Kang et al., 2019). The HMA is recognized as a global hotspot of deep stratospheric intrusion, and elevated surface

56   ozone has been observed at some ground monitoring sites and very high concentrations of surface O_3 were reported

57   (Cristofanelli et al., 2010; Yin et al., 2017; Zhu et al., 2004). At sites, it was reported that vertical ozone flux from vertical

58   transport by convective and synoptic transport was prominent in the summer at Waliguan leading to high ozone levels (Ma et

59   al., 2002; Ma et al., 2005). Studies at Shangri-La and Nam Co in HMA indicated that the input of ozone from the stratosphere

60   had potential impacts on the seasonal variations of surface ozone at each site (Yin et al., 2017; Ma et al., 2014). Still, the link

61 between the variability of surface ozone and stratospheric intrusions at the regional scale remains unclear.

62 **2. Materials and Methods**

63 **2.1. Surface measurements.**

64 This study synthesized ground measurements of surface ozone by analyzing the ground observation data collected at 16

65 sites (Fig. 1 and Table S1 in Supplementary), including 3 background sites and 13 urban sites ranging in location from the

66 southern flank of the Himalaya to the central and northeastern Tibetan Plateau. Surface ozone concentrations in 2012 at 3

67 background sites were obtained from Putero et al. (2014) and ISAC (The Institute of Atmospheric Sciences and Climate,

68 https://www.isac.cnr.it/en), Xu et al. (2020) and Yin et al. (2017). Surface ozone, nitrogen dioxide (NO_2), and carbon monoxide

69 (CO) concentrations in 2016 at 13 urban sites were provided by Geographic Data Sharing Infrastructure, College of Urban and

70 Environmental Science, Peking University (http://geodata.pku.edu.cn) and the China National Environmental Monitoring

71 Center (http://106.37.208.233:20035/). The measurements of nitrogen dioxide (NO_2) and carbon monoxide (CO) were carried

72 out at the air sampling sites run by the state, and the operation of sites followed the technical regulation for selection of ambient

73 air quality monitoring stations (National Environmental Protection Standards of the People's Republic of China, HJ 664-2013).

74 Ozone was measured with the UV-spectrophotometry method, NO_2 with the chemiluminescence method, and CO with the

75 non-dispersive infrared absorption and the gas filter correlation infrared absorption method. The specifications and test

76 procedures of NO_2, CO, and O_3 followed the Specifications and Test Procedures for Ambient Air Quality Continuous

77 Automated Monitoring System for NO_2, O_3, and CO (National Environmental Protection Standards of the People's Republic

78 of China, HJ 654-2013).

79

80

81 **Figure 1. Sixteen study sites (background sites in blue, and urban sites in purple) and their monthly mean**

82 **surface ozone variations across the High-Mountain Asia used in this study. Map of yearly mean concentration of**

83   **surface ozone in 2106 at 543.75 hPa simulated with CAM-chem is shown with colored shadings. Surface ozone data at**

84   **NCO-P, Waliguan, and Nam Co were obtained from ISAC (The Institute of Atmospheric Sciences and Climate,**

85   **https://www.isac.cnr.it/en), Xu et al. (2020), and Yin et al. (2017).**

86

87   **2.2. Reanalysis data.**

88   The ECMWF (European Centre for Medium-Range Weather Forecasts) ERA-5 data (0.28125° latitude × 0.28125°

89   longitude horizontal resolution, and 137 vertical levels) (Hoffmann et al., 2019) were used to analyze the monthly mean

90   meridional cross-section structures of troposphere and stratosphere over the HMA. Monthly mean tropopause fold was

91   investigated in this study and was defined by 2 pvu (potential vorticity unit) iso-surface and identified by the method described

92   in Luo et al. (2019).

93   **2.3. Model simulation.**

94   The Community Atmosphere Model with Chemistry (CAM-chem), a global model, was used for simulations of global

95   tropospheric and stratospheric atmospheric composition (Lamarque et al., 2012) provided by University Corporation for

96   Atmospheric Research (https://www.acom.ucar.edu/cam-chem/cam-chem.shtml). The horizontal resolution for CAM-chem is

97    $0.5° × 0.5°$. CAM-chem uses the MOZART (Model for OZone And Related chemical Tracers) chemical mechanisms

98   (Lamarque et al., 2012), with various choices of complexity for tropospheric and stratospheric chemistry. The O_{3S} variable, a

99   stratospheric ozone tracer that represents the amount of ozone in the troposphere originated in the stratosphere, in CAM-chem

100   simulation was used in this study to indicate the intensity of the ozone transported from the stratosphere (Tilmes et al., 2016).

101   O3S/O3 ratio was calculated to investigate the intensity of impacts from the stratospheric intrusion to ozone concentration in

102   troposphere.

103   **3. Results and Discussion**

104   **3.1. Surface ozone variations over HMA.**

105   The monthly mean surface ozone concentrations at 16 sites over HMA peaked in different months and moved gradually

106   from May in the south to July in the north (Fig. 1). Specifically, 8 southern sites (site No. 9-16 in Fig. 1) witnessed the ozone

107   peak in May, while the 8 northern sites (site No.1-8 in Fig. 1) have ozone peaks at June and July. It is noteworthy that such

108   regular migration of monthly ozone peaks occurred at large geographical scale, and surface ozone concentrations peaked

109   synchronously at sites in the same zone despite the differences in size of cities and baseline levels of surface ozone.

110   **3.2. Photochemical production is not likely the dominant of surface ozone.**

Atmospheric
Chemistry
and Physics
Discussions

111   The tropospheric ozone budget generally increases via two processes: influx of ozone from the stratosphere, and in-situ

112   photochemical production. The local photochemical production of ozone is generated through a chain of photochemical

113   oxidation of CO and VOCs (volatile organic compounds) catalyzed by HO_x radicals ($OH + H$ + peroxy radicals) in the presence

114   of NO_x and terminated by the loss of HO_x radicals through the oxidation of NO_2 by OH ($NO_2+OH+M \rightarrow HNO_3+M$) and the

115   self-reaction of HO_2 ($HO_2+HO_2 \rightarrow H_2O_2+O_2$). The monthly mean concentrations of surface ozone, NO_2 and CO (Supplementary,

116   Figs. S1 and S2) at urban sites in 2016 were analyzed to elucidate the contribution of in-site photochemical production. NO_2

117   and CO at several sites were negatively correlated with ozone, while there were sites with a positive correlation between ozone

118   and NO_2 (Guoluozhou, Nagqu, and Nyingchi), and between ozone and CO (Nagqu and Nyingchi). Even for the sites with

119   monthly mean concentrations of ozone negatively correlated with NO_2 and CO, the months with the highest concentration of

120   monthly mean ozone did not correspond with the months with the lowest concentration of monthly mean NO_2 and CO

121   (Supplementary, Figs. S1 and S2). Furthermore, the net ozone photochemical production was found to be negative in the

122   summer when surface ozone reached a maximum in the northeastern Tibetan Plateau (Zhu et al., 2004; Ma et al., 2002). In

123   addition, the monthly variation in surface ozone at three different types of sites in the central Tibetan Plateau (Lhasa: urban

124   site; Dangxiong: rural site; Nam Co: remote site) with varying conditions of ozone precursors were similar (Yin et al., 2017).

125   Therefore, the monthly mean surface ozone peaks in HMA were not mainly attributed to the urban photochemical production

126   of ozone.

127   **3.3. Impact of stratospheric intrusion evidenced by stratospheric ozone tracer.**

128   Rather than photochemical production, the stratospheric influx of ozone is likely a main contributor to the surface ozone

129   over HMA. This is evidenced by analysis of a stratospheric ozone tracer of O_{3S} (a stratospheric ozone tracer that represents

130   the amount of ozone in the troposphere originated in the stratosphere in CAM-chem) at 3 remote sites (NCO-P, Nam Co, and

131   Waliguan) across the south-north transection of HMA. At NCO-P in the southern Tibetan Plateau, surface ozone peaked in

132   May (Fig. 1) and it was stated that the surface ozone mixing ratios at NCO-P were significantly increased by the stratospheric

133   intrusions (+13 ppb during stratospheric intrusions) (Cristofanelli et al., 2010). At Nam Co in the central Tibetan Plateau, the

134   monthly mean mixing ratio of surface ozone peaked (ca. 60 ppb) in May (Fig. 1), while it occurred later than those at NCO-P

135   (Supplementary, Fig. S3). At Waliguan in the northern Tibetan Plateau, the monthly mean concentration of surface ozone was

136   highest in June, later than those at Nam Co and NCO-P (Fig. 1). The previous studies stated that the peak of surface ozone in

137   June at Waliguan was due to the downward transport of ozone from the upper troposphere and lower stratosphere (Ma et al.,

138   2005; Ding and Wang, 2006). We found that the high episodes of surface ozone at these 3 sites generally corresponded to high

139   O_{3S} at each site, especially during the periods with high surface ozone concentrations (spring for NCO-P and Nam Co; summer

140   for Waliguan) (Supplementary, Fig. S4). O_{3S} to O_3 ratio (O_{3S}/O_3, indicating the contribution from stratospheric ozone to surface

141   ozone) at NCO-P and Nam Co was higher in winter and spring than in summer and autumn. For Waliguan, the highest O_{3S}/O_3

142   was in July (Supplementary, Table S2). For the whole of 2012, the stratospheric intrusion of ozone contributed ~65% to the

143   surface ozone at 3 three remote sites: 63.5% at NCO-P, 64.3% at Nam Co, and 68.4% at Waliguan, which was a dominant

144   share.

145   **3.4. Additional evidences from reanalysis data and simulation.**

146   The dominant impact of stratospheric intrusion on the surface ozone can be further supported by the monthly averages of

147   the total tropopause fold frequencies (tropopause fold was indicated by 2 potential vorticity unit iso-surface, in Luo et al.,

148   (2019)) over the HMA (Fig. 2). In April, the highest frequencies of total tropopause fold were concentrated in ca. 25-30°N

149   latitude band covering parts of South Asia, the southern Tibetan Plateau, and southern China (Fig. 2). The band of high total

150   tropopause fold frequencies kept migrating northward in May, June and July, with the largest spatial coverage over the Tibetan

151   Plateau and surrounding regions in June (Fig. 2). It was found that the displacement of the tropopause fold in the Tibetan

152   Plateau was controlled by the movement of the westerly jet Luo et al. (2019). The monthly mean meridional cross-section of

153   westerly jet (indicated by the maximum speed of the U component of winds), potential vorticity, and the transport of ozone

154   from the stratosphere to the troposphere was calculated and visualized using the monthly mean ERA-5 data from April to July

155   2016 (Fig. 2). In April, the westerly jet was mainly above the Himalayas and the southern Tibetan Plateau (25-30°N), and the

156   tropopause folding mostly occurred above the southern Tibetan Plateau (Fig. 2). Both kept moving northward in May, June

157   and July, being above the southern and central Tibetan Plateau in May, above the central and northern Tibetan Plateau in June,

158   and above the northern Tibetan Plateau (~40°N) in July. The position of tropopause folding over HMA helped further

159   investigate the instruction of stratospheric air masses with high ozone concentrations to the lower troposphere and surface

160   level. The distribution of monthly mean O_{3S} at 543.75 hPa in 2016 over HMA obtained from CAM-chem simulations indicated

161   that O_{3S} in the southern Tibetan Plateau reached its maxima in May, whereas O_{3S} in the northern Tibetan Plateau was higher

162   in both June and July than in April and May (Supplementary, Fig. S5). The pattern of O_{3S} simulated with CAM-chem supported

163   with the analysis of tropopause fold and meridional cross-section using the ERA-5 data. Therefore, CAM-chem clearly

164   demonstrated that the westerly jet and the tropopause fold moved from the southern Tibetan Plateau to the northern Tibetan

165   Plateau from April to July, and the meridional transition of the tropopause fold from south to north led to the migration of

166   stratospheric intrusions of ozone progressively from south to north affecting the concentrations of surface ozone at various

167   sites across HMA.

168
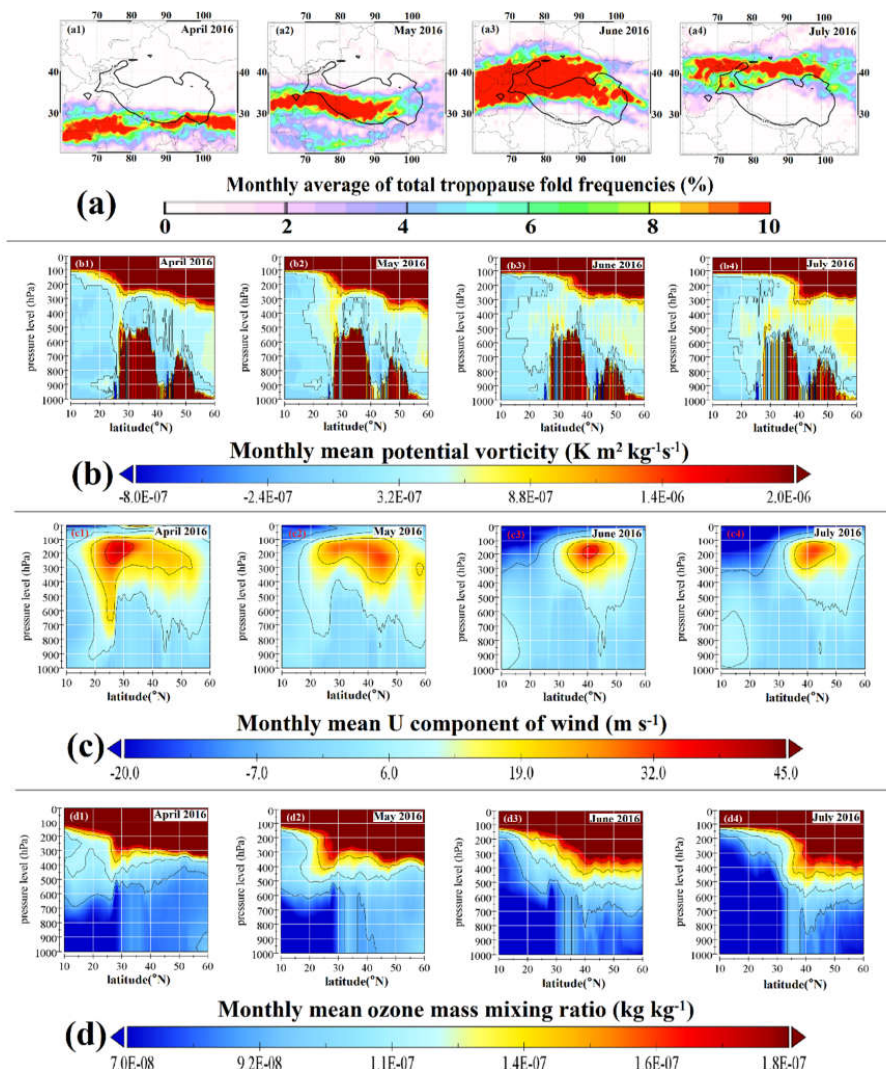
Figure 2. Monthly average of total tropopause fold frequencies (a) in April, May, June, and, July in 2016. Monthly mean meridional cross-section of ERA-5 data at 91°E (~ the central Tibetan Plateau) showing the potential vorticity (b), zonal winds c), and ozone mass mixing ratio(d) in April, May, June, and, July in 2016. The location of the Tibetan Plateau (main body of High-Mountain Asia, 3 km elevation) is shown with black contour in the maps.

4. Conclusions.

The ground measurements of surface ozone at 16 sites (3 remote and 13 urban sites) spread across the Tibetan Plateau, the main body of HMA, were used for the first time in this study, as opposed to previous studies which focused mostly on

178 individual sites. Simulation results from CAM-chem and analysis of ERA-5 reanalysis data were used to investigate the

179 influence of the downward influx of ozone from the stratosphere on the variation in surface ozones. Results showed that the

180 peak in monthly mean surface ozone concentration occurs first over the southern Tibetan Plateau in April. The peak then moves

181 progressively northwards in later summer in conjunction with the similar northward movement of the tropopause folds and

182 westerly jet, which act as the two main control mechanisms. The position of tropopause folds was controlled by the position

183 of the westerly jet and created the conditions conducive for the influx of ozone rich air from the deep stratosphere to the

184 troposphere. The migration of the folds led to a similar migration from south to north of stratospheric intrusions. This lead to

185 a dominant contribution of stratospheric intrusions to the surface ozone (~65% at remote background sites), elevating the

186 baseline (background) ozone concentrations as well as peak concentrations during high-ozone episodes. We suggest that the

187 transport of stratospheric ozone to the surface is a regionally coherent dominant contributor to surface ozone across the HMA,

188 which needs a proper consideration in understanding the atmospheric chemistry and the impacts of ozone over this highland

189 region and beyond.

190

191

199 **Data Availability Statement:** The surface ozone data at Nam Co, Waliguan, and NCO-P in this study are available through

200 Yin et al. (2017), Xu et al. (2020), Putero et al. (2014), and ISAC (The Institute of Atmospheric Sciences and Climate,

201 https://www.isac.cnr.it/en). Surface ozone, NO_2, and CO data at 13 urban sites are available through Geographic Data Sharing

202 Infrastructure, College of Urban and Environmental Science, Peking University (https://geodata.pku.edu.cn/index.php?c=

203 content&a=show&id=1730#, after login). ERA-5 data are available through the European Centre for Medium-Range Weather

204 Forecasts (https://cds.climate.copernicus.eu/cdsapp#!/dataset/reanalysis-era5-single-levels?tab=form, after login). CAM-

205 chem data are available through University Corporation for Atmospheric Research (https://www.acom.ucar.edu/cam-

206 chem/cam-chem.shtml).

207

208 **Author contributions: Xiufeng Yin:** Conceptualization, visualization, writing - original draft. **Benjamin de Foy, Dipesh**

209 **Rupakheti, Zhenming Ji, Zhiyuan Cong, Guoshuai Zhang, and Maheswar Rupakheti:** Writing - review & editing.

210 **Junhua Yang and Ping Li:** Visualization. **Jiali Luo:** Visualization, writing – review. **Shichang Kang, Qianggong Zhang:**

211 Conceptualization, writing - review & editing.

212 **Competing interests**

213 The authors declare no competing interests.

214

215 **References**

216 Bracci, A., Cristofanelli, P., Sprenger, M., Bonafè, U., Calzolari, F., Duchi, R., Laj, P., Marinoni, A., Roccato, F., and

217   Vuillermoz, E.: Transport of Stratospheric Air Masses to the Nepal Climate Observatory–Pyramid (Himalaya; 5079 m

218   MSL): A Synoptic-Scale Investigation, Journal of applied meteorology and climatology, 51, 1489-1507, 2012.

219 Cristofanelli, P., Bracci, A., Sprenger, M., Marinoni, A., Bonafè, U., Calzolari, F., Duchi, R., Laj, P., Pichon, J. M., Roccato,

220   F., Venzac, H., Vuillermoz, E., and Bonasoni, P.: Tropospheric ozone variations at the Nepal Climate Observatory-

221   Pyramid (Himalayas, 5079 m a.s.l.) and influence of deep stratospheric intrusion events, Atmospheric Chemistry and

222   Physics, 10, 6537-6549, 10.5194/acp-10-6537-2010, 2010.

223 Crutzen, P. J.: Tropospheric ozone: An overview, Tropospheric ozone, 3-32, 1988.

224 Ding, A., and Wang, T.: Influence of stratosphere-to-troposphere exchange on the seasonal cycle of surface ozone at Mount

225   Waliguan in western China, Geophysical research letters, 33, 2006.

226 Hoffmann, L., Günther, G., Li, D., Stein, O., Wu, X., Griessbach, S., Heng, Y., Konopka, P., Müller, R., and Vogel, B.: From

227   ERA-Interim to ERA5: the considerable impact of ECMWF's next-generation reanalysis on Lagrangian transport

228   simulations, Atmospheric Chemistry and Physics, 19, 3097-3124, 2019.

229 Kang, S., Zhang, Q., Qian, Y., Ji, Z., Li, C., Cong, Z., Zhang, Y., Guo, J., Du, W., and Huang, J.: Linking atmospheric pollution

230   to cryospheric change in the Third Pole region: current progress and future prospects, National Science Review, 6, 796-

231   809, 2019.

232 Lamarque, J. F., Emmons, L. K., Hess, P. G., Kinnison, D. E., Tilmes, S., Vitt, F., Heald, C. L., Holland, E. A., Lauritzen, P.

233   H., Neu, J., Orlando, J. J., Rasch, P. J., and Tyndall, G. K.: CAM-chem: description and evaluation of interactive

234   atmospheric chemistry in the Community Earth System Model, Geosci. Model Dev., 5, 369-411, 10.5194/gmd-5-369-

235   2012, 2012.

236 Luo, J., Liang, W., Xu, P., Xue, H., Zhang, M., Shang, L., and Tian, H.: Seasonal Features and a Case Study of Tropopause

237   Folds over the Tibetan Plateau, Advances in Meteorology, 2019, 2019.

238 Ma, J., Liu, H., and Hauglustaine, D.: Summertime tropospheric ozone over China simulated with a regional chemical transport

239   model 1. Model description and evaluation, Journal of Geophysical Research: Atmospheres, 107, ACH 27-21-ACH 27-

240   13, 2002.

241 Ma, J., Zheng, X., and Xu, X.: Comment on "Why does surface ozone peak in summertime at Waliguan?" by Bin Zhu et al,

242   Geophysical research letters, 32, 2005.

243 Ma, J., Lin, W. L., Zheng, X. D., Xu, X. B., Li, Z., and Yang, L. L.: Influence of air mass downward transport on the variability

244   of surface ozone at Xianggelila Regional Atmosphere Background Station, southwest China, Atmospheric Chemistry and

245   Physics, 14, 5311-5325, 10.5194/acp-14-5311-2014, 2014.

246 Putero, D., Landi, T. C., Cristofanelli, P., Marinoni, A., Laj, P., Duchi, R., Calzolari, F., Verza, G. P., and Bonasoni, P.:

247   Influence of open vegetation fires on black carbon and ozone variability in the southern Himalayas (NCO-P, 5079 m

248   a.s.l.), Environ Pollut, 184, 597-604, 10.1016/j.envpol.2013.09.035, 2014.

249 Tilmes, S., Lamarque, J. F., Emmons, L. K., Kinnison, D. E., Marsh, D., Garcia, R. R., Smith, A. K., Neely, R. R., Conley, A.,
250   Vitt, F., Val Martin, M., Tanimoto, H., Simpson, I., Blake, D. R., and Blake, N.: Representation of the Community Earth
251   System Model (CESM1) CAM4-chem within the Chemistry-Climate Model Initiative (CCMI), Geosci. Model Dev., 9,
252   1853-1890, 10.5194/gmd-9-1853-2016, 2016.

253 Xu, X., Lin, W., Xu, W., Jin, J., Wang, Y., Zhang, G., Zhang, X., Ma, Z., Dong, Y., and Ma, Q.: Long-term changes of regional
254   ozone in China: implications for human health and ecosystem impacts, Elem Sci Anth, 8, 2020.

255 Yao, T., Thompson, L., Yang, W., Yu, W., Gao, Y., Guo, X., Yang, X., Duan, K., Zhao, H., and Xu, B.: Different glacier
256   status with atmospheric circulations in Tibetan Plateau and surroundings, Nature Climate Change, 2, 663-667, 2012.

257 Yin, X., Kang, S., de Foy, B., Cong, Z., Luo, J., Zhang, L., Ma, Y., Zhang, G., Rupakheti, D., and Zhang, Q.: Surface ozone
258   at Nam Co in the inland Tibetan Plateau: variation, synthesis comparison and regional representativeness, Atmospheric
259   Chemistry and Physics, 17, 11293-11311, 10.5194/acp-17-11293-2017, 2017.

260 Zhu, B., Akimoto, H., Wang, Z., Sudo, K., Tang, J., and Uno, I.: Why does surface ozone peak in summertime at Waliguan?,
261   Geophysical research letters, 31, 2004.

262
263